RSC Advances

PAPER

View Article Online
View Journal | View Issue

Cite this: *RSC Adv.*, 2020, **10**, 29737

Metallic SPIONP/AgNP synthesis using a novel natural source and their antifungal activities

Sara Azhdari,[ab] Roghayeh Ershad Sarabi,[c] Nadia Rezaeizade,[d] Faride Mosazade,[a] Mohammadjavad Heidari,[e] Fariba Borhani,*[f] Meghdad Abdollahpour-Alitappeh[g] and Mehrdad Khatami*[ah]

Received 6th May 2020
Accepted 6th July 2020

DOI: 10.1039/d0ra04071a

rsc.li/rsc-advances

The green synthesis of nanoparticles (NPs) is important because of the favorable potential of plant biomolecules involved in the synthesis of NPs. This study aimed to provide a fast, easy, cheap, and environmentally friendly method for the synthesis of superparamagnetic iron oxide NPs (SPIONP) and silver nanoparticles (AgNPs) using *Stachys lavandulifolia* and an evaluation of their use as antifungal agents against *Aspergillus niger* and *Fusarium solani*. The physicochemical properties of AgNPs and SPIONPs were studied using FESEM, HRTEM, XRD, VSM, UV-Vis, and EDX spectroscopy. The sizes and morphologies of the AgNPs and SPIONPs, measured *via* electron microscopy, were 12.57 nm and 10.70 nm, respectively. Nanoparticles have previously been shown to have antifungal activities, and SPIONPs and AgNPs can show antifungal resistance. These NPs can be used as a substitute for widely used toxic fungicides to promote food safety and public health.

Introduction

Nanotechnology examines the properties of materials that have at least one dimension smaller than 100 nm,[1] so that the physical, chemical, and biological properties of these particles differ substantially from those of their bulkier samples.[2–5] Currently, NPs are mainly produced using a variety of physicochemical methods that have disadvantages such as low stability, dependence on advanced equipment, high temperature, high pressure and the production of toxic by-products with adverse effects on the environment.[6,7] Considering the problems mentioned in previous approaches, the discovery of inexpensive and environmentally friendly methods for the production of NPs is essential.[8–11] The green nanoparticle synthesis method uses fungi, bacteria, algae, and plants, which are considered the most inexpensive and accessible plants and do not require specific conditions or a complex culture environment to grow.[12] In the green synthesis method, plant extracts of NPs may contain many secondary compounds and metabolites.[13]

An increasing resistance of pathogens to antimicrobial agents such as fungicides and antibiotics has become a global problem.[14–17] Nanoparticles have various applications in medicine for controlling disease and in other fields.[18] The AgNPs and SPIONPs are the most widely studied and they have unique physical, chemical, and biological properties, and their antimicrobial activity has been demonstrated.[19–22] Magnetic NPs with unique properties of biocompatibility and biodegradability are increasingly being used in research and for various applications in science and technology, including biosensors, water treatment, MRI imaging, targeted transfer and targeted drugs.[23–25] Because of their specific properties, they can interact with different microorganisms without posing a risk to human health. Various types of compounds and iron oxides exist in nature including Fe_3O_4 and Fe_2O_3.[9] Nanoparticles have a higher antimicrobial activity against pathogens with higher surface-to-volume ratios than their bulk materials and can be used as a viable strategy in control of microorganisms.[26,27] Although there are numerous studies on the antimicrobial properties of nanomaterials, their mechanism in the control of microbes is not yet well understood. Studies show that AgNPs bind to the phosphorus groups on DNA, causing the DNA to become more compact and prevent its proliferation and cell death. The AgNPs can also cause deformation and damage to the hyphae structure. The SPIONPs can interact with microbial cells and cause damage to cell membranes, as well as the destruction of

[a]*Noncommunicable Diseases Research Center, Bam University of Medical Sciences, Bam, Iran*
[b]*Department of Anatomy and Embryology, School of Medicine, Bam University of Medical Sciences, Bam, Iran*
[c]*Department of Health Information Sciences, Faculty of Management and Medical Information Sciences, Kerman University of Medical Sciences, Kerman, Iran*
[d]*Clinical Research Center, Pastor Educational Hospital, Bam University of Medical Sciences, Bam, Iran*
[e]*Faculty of Pharmacy, Cyprus International University, Lefkosa, Turkish Republic of Northern Cyprus, Lefkosa, Cyprus*
[f]*Medical Ethics and Law Research Center, Shahid Beheshti University of Medical Sciences, Tehran, Iran. E-mail: faribaborhani@msn.com*
[g]*Cellular and Molecular Biology Research Center, Larestan University of Medical Sciences, Larestan, Iran*
[h]*Cell Therapy and Regenerative Medicine Comprehensive Center, Kerman University of Medical Sciences, Kerman, Iran*

macromolecules and the production of O_2 super peroxidase. In this study, a leaf extract of *Stachys lavandulifolia* was used, which is one of the important medicinal plants of the Lamiaceae family because its extract contains polyphenol and flavonoid compounds.

For the cases captured in this study, the extract and *S. lavandulifolia* were used for synthesis of AgNPs and SPIONPs, respectively, and their antifungal effects against two strains of pathogenic fungi were investigated.

Materials and methods

Preparation of the plant extract

The leaves were collected from *S. lavandulifolia* and these were dried and subjected to extraction after powdery mildew formed. The extract from *S. lavandulifolia* leaves was extracted before the flowering stage, and the leaves were washed with deionized water to remove the dust from the leaf surface. The leaves were dried in shade and at room temperature for four days and then the leaves were powdered in a sterilized mortar and kept in a closed container away from moisture and light at room temperature until required. Then, 20 ml of deionized water was added to each gram of extract powder and stirred at 60 °C on a heated stirrer at 360 rpm for 1 h followed by filtration using Whatman® Cellulose Filter Paper No. 42 and the filtrate was then centrifuged at 4 °C for 95 min at 9500 rpm. Finally, the supernatant was filtered and centrifuged again with the same Whatman paper. The extract was stored in the dark at 4 °C and sterile media was used at all stages.

Green synthesis of silver and iron nanoparticles

For the green synthesis of AgNPs, a 100 mM silver nitrate storage solution was first prepared and 1 ml of the plant extract was added to 2 ml micro-tubes and the contents of each micro-tube was diluted to find the appropriate concentration of silver nitrate for the synthesis of AgNPs. A portion of the stored silver nitrate solution (20, 25, 30, 35, 40, 45, 50, 55 or 60 μl) was added to the contents of the tube and the reaction mixture was kept at ambient temperature and the color change of the plant extract was investigated at different times. The AgNPs were precipitated using a centrifuge. The precipitate of AgNPs was collected by centrifugation at 14 000 rpm for 15 min, washed twice with deionized water to remove the unreacted materials and impurities, and then finally washed with absolute ethanol. The collected powder was dried at 60 °C.

The SPIONPs, 41 mM $FeCl_3$ and 27 mM $FeCl_2$ (1 : 1.5) were first dissolved in deionized water in a sterile Erlenmeyer flask with a lid which was completely closed and then shaken well on a heated stirrer. When the temperature reached 80 °C, the plant extract was added, and after 10 min, it was adjusted to pH 11 with 1 M sodium hydroxide and then centrifuged three times after cooling (12 000 rpm, 15 min, 4 °C) with the removal of the solid residue. The resulting supernatant was dried for 24 h at 80 °C on glass and the powder obtained was used to determine the characteristics of the synthesized NPs and their biological activity.

Characterization of the nanoparticles

Ultraviolet absorption of the synthesized nanoparticles was investigated using a UV-Vis Drop 250-211Fo75 spectrophotometer (Germany). The crystalline structure of the powdered samples was examined using XRD with the X'Pert PRO (PANalytical, Netherlands). Scanning electron microscopy (SEM) was performed using a Sigma VP (Carl Zeiss) to determine the morphological properties of the NPs. To determine the exact size and shape of the synthesized nanoparticles, a transmission electron microscope (TEM, FEI Tecnai) was used. The magnetic properties of the SPIONPs were investigated using a vibrating sample magnetometer (VSM, Lake Shore-7400, Lake Shore Cryonics, USA).

Antifungal effects of AgNPs and SPIONPs

In order to investigate the biological activity of the AgNPs and SPIONPs on the growth of fungi, two strains of fungi: *Aspergillus niger* and *Fusarium solani* were propagated in potato dextrose agar (PDA) medium. For the iron NPs, 0.1 g of the NP powder was first dissolved in 10 ml of deionized water and sonicated (probe 6 mm, 10% ambient, 60 s sonic and 15 s rest and then repeated 15 times) to disperse the NPs. The AgNPs and SPIONPs at concentrations of 0, 1, 5, 25, or 50 ppm were added to 20 ml of PDA medium immediately after autoclaving. From the new cultures of the tested fungal strains, 5 mm discs were generated on Petri dishes and then stored at 25 °C, and the fungal radial growth was measured after 24 h and 48 h.

Statistical analysis

Statistical analysis was performed in a completely randomized design with a factorial arrangement with three replications and the data were analyzed using SPSS version 25 software (IBM). The comparison of means was performed by a Duncan test at the significant level of 0.01.

Results

The discoloration of the extract to brown after the addition of silver nitrate (less than 1 h) and the change of the color of the solution containing iron salts from yellow to charcoal were the first indications of the production of AgNPs and SPIONPs. To

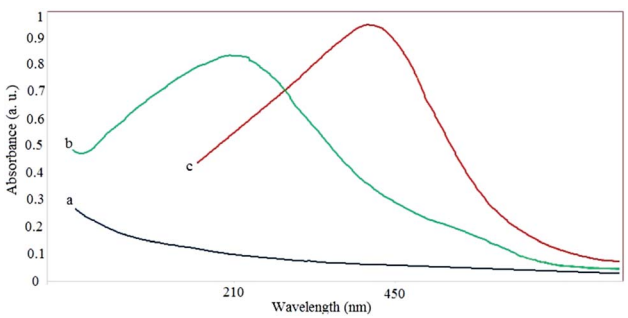

Fig. 1 Absorption spectra of plant extract (a), SPIONPs (b) and AgNPs (c).

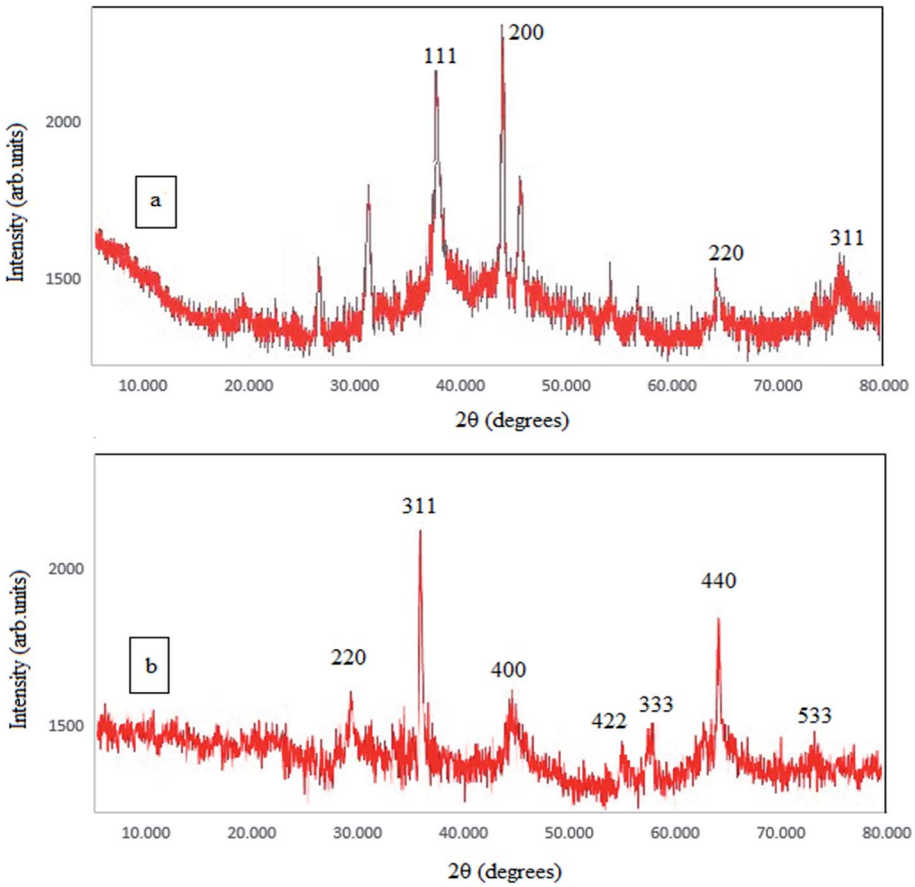

Fig. 2 The XRD spectra of AgNPs (a) and SPIONPs (b) synthesized with *Stachys lavandulifolia* extract.

confirm the formation of NPs and their presence, the solutions were analyzed by a spectrophotometric method. Fig. 1 shows the UV-Vis spectra of the AgNPs and the SPIONPs. These spectra indicate that a high adsorption occurred at 432 nm and 212 nm for AgNPs and SPIONPs, respectively, whereas the plant extract lacked an absorption peak.

X-ray diffraction ($2\theta = 10^{\circ}$ to 80°) was used in this study to study the crystal structure of the synthesized NPs and to re-

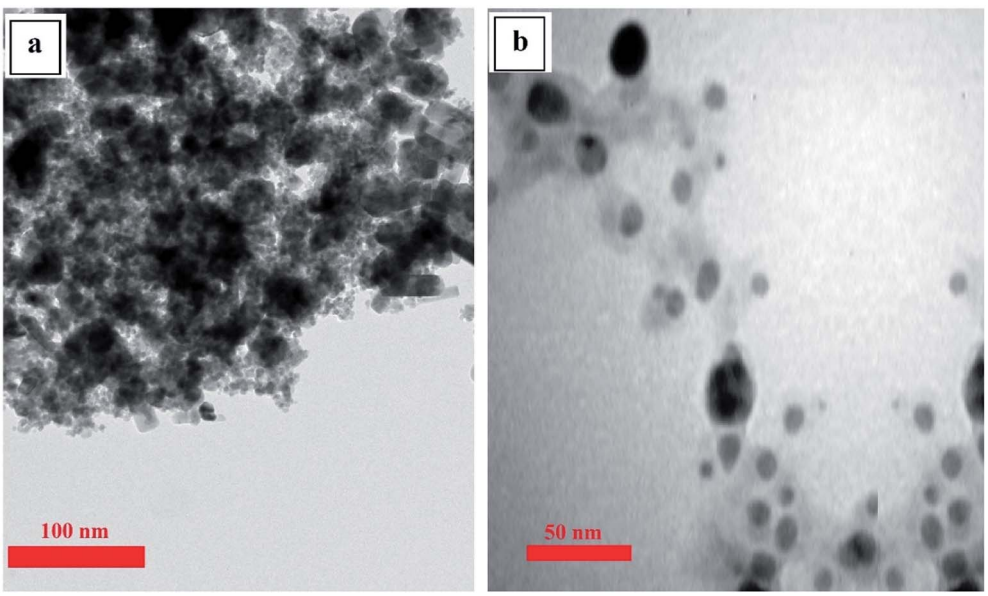

Fig. 3 TEM images of SPIONPs (a) and AgNPs (b) synthesized with *Stachys lavandulifolia* extract.

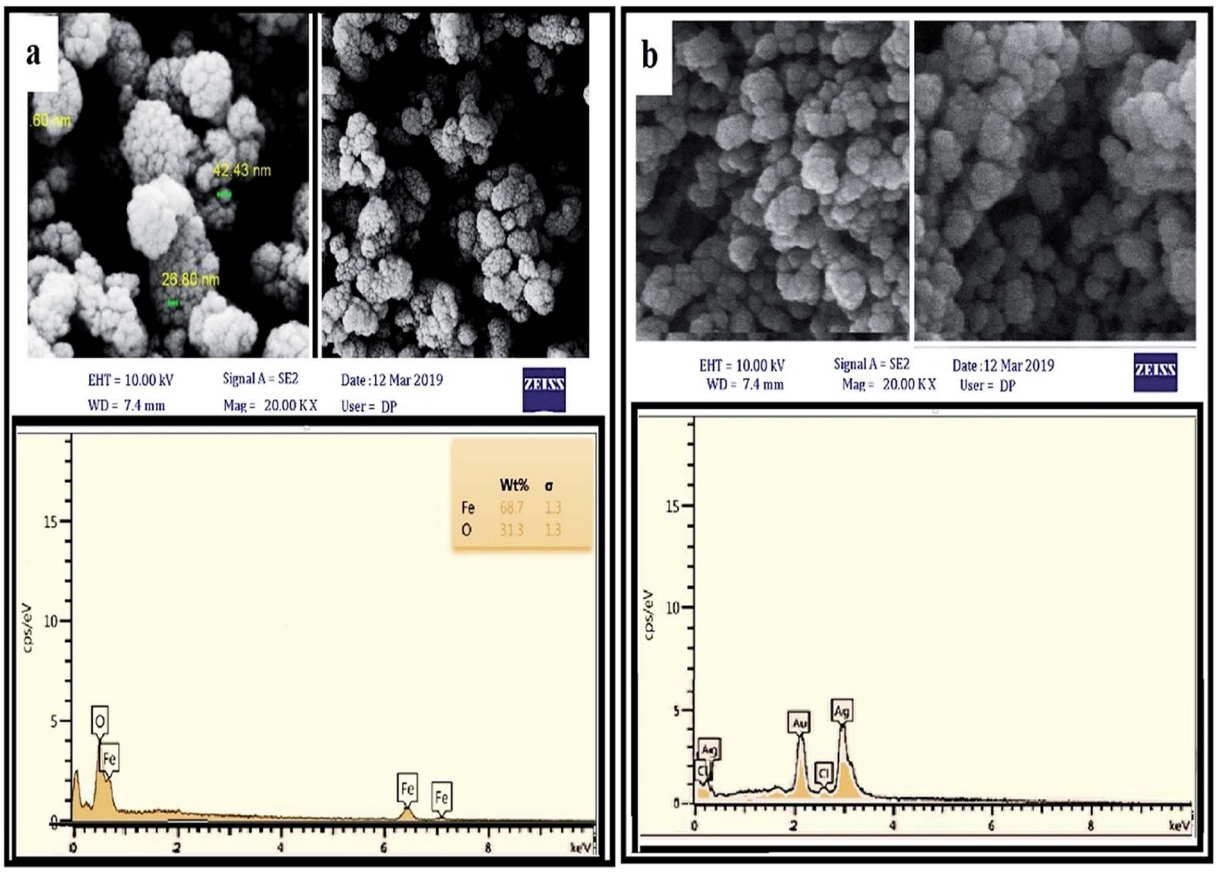

Fig. 4 FESEM and EDX images of SPIONPs (a) and AgNPs (b) synthesized with *Stachys lavandulifolia* extract.

confirm the synthesis of the NPs. As shown in the Fig. 2, clear peaks are shown for SPIONPs at $2\theta = 30.47, 35.77, 43.49, 53.85, 57.33, 62.9, 74.37$ (inverse spinel cubic structure) and for AgNPs at $2\theta = 27.85, 32.21, 38.08, 44.3, 46.2, 64.45, 77.29$ (the face centered cubic structure).[28] The Scherrer formula (eqn (1)) was used for determining the size of the NPs. The crystallite size of the NPs (diameter) was estimated to be about 11.56 nm and 13.05 nm, for AgNPs and SPIONPs, respectively.

$$\tau = \frac{K\lambda}{\beta \cos \theta} \quad (1)$$

where, τ is the crystallite size (nm), K is the crystallite shape coefficient (0.9), λ is the X-ray generator wavelength (0.154 nm), β is the FWHM, and θ is the diffraction angle.

Transmission electron microscopy was used to determine the size, shape, and distribution of the synthesized nanoparticles,[29] and the results (Fig. 3) show that both of the synthesized NPs are spherical particles and have an average size of less than 50 nm.

The surface morphology and chemical composition of the NPs were determined by FESEM (Fig. 4). The FESEM images also confirm that the distribution of particles was uniform and that they had the same spherical shape. As can be seen in the EDX spectrum, the SPIONPs were composed of only Fe and O (100% total) and the AgNPs were mainly composed of Ag and Cl, and the results confirmed the purity of the synthesized NPs. The presence of peaks at 0.6 and 6.5 keV for SPIONPs and 3 keV for AgNPs was observed due to SPR and confirmed the synthesis of the NPs.

VSM was used to investigate the magnetic properties of the SPIONPs. The curve shows the residual curve of the Fe_3O_4

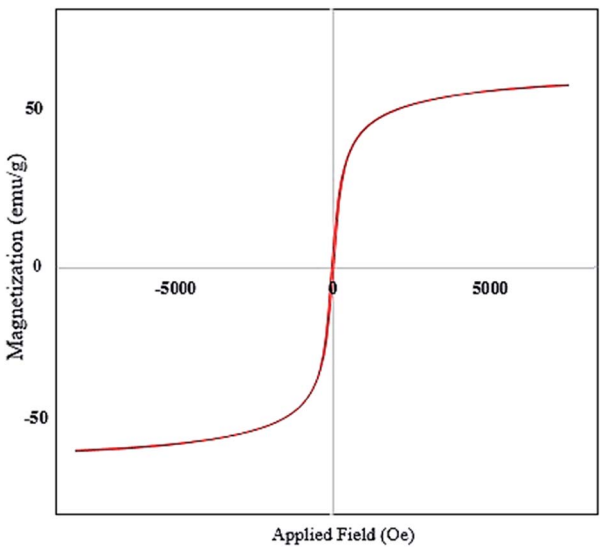

Fig. 5 VSM curve of SPIONPs synthesized with *Stachys lavandulifolia* extract (emu: electromagnetic units).

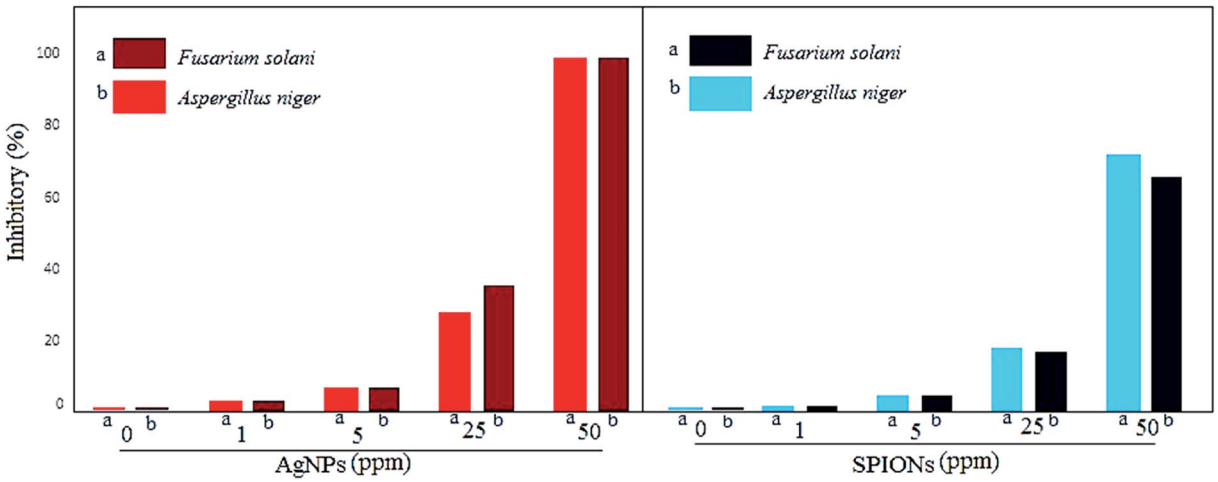

Fig. 6 The inhibitory effects of AgNPs and SPIONPs on the radial growth of the mycelia of *A. niger* and *F. solani*.

sample in the −20 000 to 20 000 Oe applied field range. The saturation magnetization curve was estimated to be 33.02 emu g^{-1}, with particle magnetization passing through the source where no residual magnetism was observed, and the force field was calculated to be 0.34 Oe (Fig. 5).

The antifungal activity of the greener synthesized NPs against two pathogenic fungi was determined by measuring the radial growth of the mycelium. The synthesized NPs showed an inhibitory effect on the radial growth of the mycelium of *A. niger* and *F. solani* (Fig. 6 and 7). In this study, AgNPs were also used to compare the antimicrobial activity of magnetic NPs of iron. It was found that AgNPs and SPIONPs were capable of inhibiting the growth of mycelia of the two fungi used in this study. A mean comparison test showed that the antifungal activity and inhibitory effect of AgNPs and SPIONPs on radial growth of mycelium of *A. niger* and *F. solani* did not show significant differences at different times and showed similar effects. The maximum inhibitory effect of AgNPs and SPIONPs on the radial growth of the fungi tested in this study was at 25 and 50 ppm, respectively.

Discussion

Metallic nanoparticles (silver and iron) are of great interest because of their many properties and applications. *Stachys lavandulifolia* is a valuable aromatic herb and is well known for its thymol and carvacrol monoterpenoids and is a good source of antioxidants. This study is the first report of the synthesis of SPIONPs from leaf extracts of this plant. The use of bio-sources as reducing agents and NPs has been widely recognized in recent decades due to their easy availability, environmental friendliness and their biocompatibility.[30,31] The discoloration of the ion-containing solution after the addition of the plant extract was the first indication of the synthesis of NPs, which was because the nanoparticles are confined to a small space as compared to a small amount of plasmonic oscillating material, leading to the effect. Surface plasmon resonance on the surface results in the color of the nanoparticles being different from their clumped state. The presence of clear peaks in the UV-Vis absorption spectrum of AgNPs and SPIONPs and their absence in the plant extract indicated the synthesis of NPs in the desired solution.[32,33] According to the theory of quantum confinement, the wavelength decreases as the particle size decreases. This spectrum again confirms the nanometer particle size and is consistent with the results of previous studies. In the XRD results, the presence of sharp peaks indicates a high degree of crystallinity for the NPs, confirming the synthesis of the NPs and it is consistent with the results of other studies. The recorded TEM images show that the conditions applied to the reduction of iron and silver ions and the green synthesis of the NPs caused AgNPs and SPIONPs to be synthesized with an average diameter of 12.57 nm and 10.70 nm, respectively, with the *S. lavandulifolia* extract. As shown in Fig. 3, the AgNPs and SPIONPs were predominantly spherical and regular, and this was fully consistent with the results of the XRD and the SEM. The strong peaks in the EDS and XRD spectra show that NPs have been synthesised and their purity. The synthesized NPs have the ability to rapidly adsorb to the magnets, and after the NPs are absorbed onto the magnets, the aqueous phase is completely transparent, indicating that no plant extract remains and all the extract used for the synthesis of the NPs has been used. After removal of the external magnetic field, the NPs were readily dispersed, which indicated that the NPs could be applied in various fields and that the iron NPs could be removed after use. According to the VSM results, the very small coercivity field could be due to the small size of the NPs and the single magnetite domain. Therefore, this curve confirms the SPIONPs superparamagnetic characteristic. Hyperparamagnetic properties are important for various applications such as in MRI and gene transfer, drug delivery, and so on, and their small size and spherical shape give better interaction with cell membranes and the antimicrobial activity of the NPs. Previous studies have reported the presence of secondary compounds in *S. lavandulifolia* leaves, and the results of FTIR show the presence of strong peaks for these compounds which confirmed the existence of different functional groups of the plant extract. The *S. lavandulifolia* is involved in the synthesis,

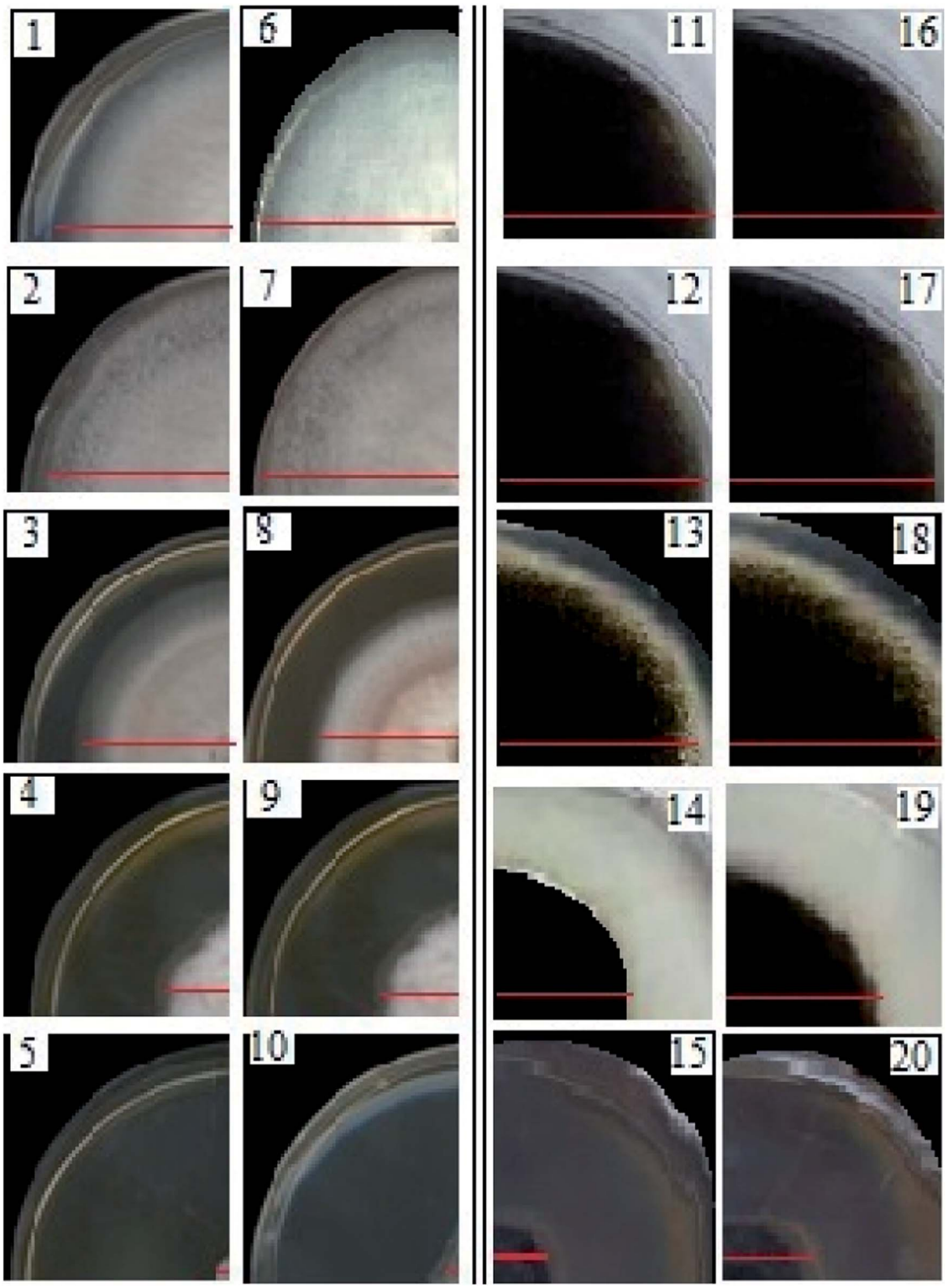

Fig. 7 The inhibitory effects of AgNPs on the mycelial growth of *F. solani* (1–5) and *A. niger* (11–15), and the inhibitory effects of SPIONPs on the mycelia growth of *F. solani* (6–10) and *A. niger* (16–20).

coating, stabilization and inhibition of NP agglomeration. For SPIONPs, the strong absorption band at 569.80 nm could be related to Fe–O and the synthesis of the SPIONPs. The observed bands were in agreement with those found in other studies.

The higher the concentration of AgNPs and SPIONPs, the greater the decrease in mycelial growth and the greater the inhibitory effect of NP growth was observed. In the case of SPIONPs, the concentration of 10 ppm is twice that of 5 ppm,

but its inhibitory effect does not differ by 5 ppm because the NPs may be agglomerated to magnetic SPIONPs at higher concentrations, therefore, for the maximum inhibitory effect of the magnetite iron NPs, the optimum amount of NPs determines the maximum antitumor effect. The size of the NPs affects their antimicrobial activity, and the smaller the NPs are, the easier it is for them to cross the cell membrane and enter the cell space, causing cell death through oxidative stress and also by affecting the macromolecules.[34] The antimicrobial properties of the NPs depends on the size, particle type, and strain of the bacterium and the fungus. There are many studies on the antimicrobial activity of SPIONPs and AgNPs, and the results of these are in line with the results of this study. Previous studies showed by producing TEM images of mycelium treated with AgNPs, that the NPs destroyed the cell membrane and inhibited the natural growth of the mycelium. Mishra *et al.*[23] highlighted the role of Fe^{2+} ions in hydrogen peroxide production and damage to macromolecules. Mishra *et al.* also demonstrated the antifungal activity of AgNPs against the pathogenic fungus. Studies have shown that AgNPs are capable of producing ROS that affect gene expression, apoptosis and cell signaling pathways. Because of their high volume, NPs are better able to interact with microorganisms and reduce the oxygen demand of cells. Although NPs have a detrimental effect on microorganisms, other studies have shown that they also have a positive effect. Silver and iron NPs have been found to have a positive effect on root length, plant growth and disease control of plants, so NPs can be an interesting alternative for plant protection and as nano-fertilizers and nano-fungicides.[35,36] Nanoparticles have been considered as an alternative in various biological applications due to their unique properties despite their bulk. Iron is a microelement required for plant growth and a plant can use the iron NPs used in a foliar spray to control fungi and pathogenic bacteria, to help plant growth and stress resistance.

Conclusions

In this study, a one-step method using cheap, easily available, and non-toxic reducing agents to reduce iron and silver ions and to synthesize AgNPs and SPIONPs, which had antifungal activities, was demonstrated. TEM and FESEM images show spherical AgNPs and SPIONPs with average sizes of 12.57 nm and 10.70 nm, respectively. FTIR spectra show the presence of plant extract biomolecules and their ability to coat the synthesized nanoparticles. In addition, both types of synthesized nanoparticles showed inhibitory effects against the radial growth of the mycelia of the pathogenic fungi *A. niger* and *F. solani*. Therefore, given the reports that some pathogens are resistant to fungicides and the need to develop other alternatives, nanoparticles synthesized from extracts of *S. lavandulifolia* may contribute to the development of new fungicides and, thus, to the management of plant diseases.

Author contributions

The authors read and approved the final manuscript.

Conflicts of interest

The authors confirm that the content of this article involves no competing interests.

Acknowledgements

The authors are thankful to the Shahid Beheshti University of Medical Sciences and Bam University of Medical Sciences for providing research facilities and finance.

References

1 M. Safaei, M. M. Foroughi, N. Ebrahimpoor, S. Jahani, A. Omidi and M. Khatami, A review on metal-organic frameworks: synthesis and applications, *TrAC, Trends Anal. Chem.*, 2019, **118**, 401–425.
2 A. Miri, N. Mahdinejad, O. Ebrahimy, M. Khatami and M. Sarani, Zinc oxide nanoparticles: biosynthesis, characterization, antifungal and cytotoxic activity, *Mater. Sci. Eng., C*, 2019, **104**, 109981.
3 G. Nagaraju, K. Karthik and M. Shashank, Ultrasound-assisted Ta_2O_5 nanoparticles and their photocatalytic and biological applications, *Microchem. J.*, 2019, **147**, 749–754.
4 R. Torkzadeh-Mahani, M. M. Foroughi, S. Jahani, M. Kazemipour and H. Hassani Nadiki, The effect of ultrasonic irradiation on the morphology of NiO/Co_3O_4 nanocomposite and its application to the simultaneous electrochemical determination of droxidopa and carbidopa, *Ultrason. Sonochem.*, 2019, **56**, 183–192.
5 T. Iranmanesh, M. M. Foroughi, S. Jahani, M. Shahidi Zandi and H. Hassani Nadiki, Green and facile microwave solvent-free synthesis of CeO_2 nanoparticle-decorated CNTs as a quadruplet electrochemical platform for ultrasensitive and simultaneous detection of ascorbic acid, dopamine, uric acid and acetaminophen, *Talanta*, 2020, **207**, 120318.
6 A. Akbari, M. Khammar, D. Taherzadeh, A. Rajabian, A. Khorsand Zak and M. Darroudi, Zinc-doped cerium oxide nanoparticles: sol-gel synthesis, characterization, and investigation of their in vitro cytotoxicity effects, *J. Mol. Struct.*, 2017, **1149**, 771–776.
7 J. A. Dahl, B. L. S. Maddux and J. E. Hutchison, Toward Greener Nanosynthesis, *Chem. Rev.*, 2007, **107**(6), 2228–2269.
8 H. Mirzaei and M. Darroudi, Zinc oxide nanoparticles: biological synthesis and biomedical applications, *Ceram. Int.*, 2017, **43**(1, part B), 907–914.
9 M. Khatami, H. Q. Alijani, B. Fakheri, M. M. Mobasseri, M. Heydarpour, Z. K. Farahani, *et al.*, Super-paramagnetic iron oxide nanoparticles (SPIONs): greener synthesis using Stevia plant and evaluation of its antioxidant properties, *J. Cleaner Prod.*, 2019, **208**, 1171–1177.
10 Y. Dağlıoğlu and B. Yılmaz Öztürk, A novel intracellular synthesis of silver nanoparticles using Desmodesmus sp. (Scenedesmaceae): different methods of pigment change, *Rendiconti Lincei. Sci. Fis. Nat.*, 2019, **30**(3), 611–621.
11 F. T. Minhas, G. Arslan, I. H. Gubbuk, C. Akkoz, B. Y. Ozturk, B. Asıkkutlu, *et al.*, Evaluation of antibacterial properties on

polysulfone composite membranes using synthesized biogenic silver nanoparticles with Ulva compressa (L.) Kütz. and Cladophora glomerata (L.) Kütz. extracts, *Int. J. Biol. Macromol.*, 2018, **107**, 157–165.

12 P. Singh, Y.-J. Kim, D. Zhang and D.-C. Yang, Biological Synthesis of Nanoparticles from Plants and Microorganisms, *Trends Biotechnol.*, 2016, **34**(7), 588–599.

13 S. Ahmed, M. Ahmad, B. L. Swami and S. Ikram, A review on plants extract mediated synthesis of silver nanoparticles for antimicrobial applications: a green expertise, *J. Adv. Res.*, 2016, **7**(1), 17–28.

14 C. L. Ventola, The Antibiotic Resistance Crisis: Part 1: Causes and Threats, *Pharm. Ther.*, 2015, **40**(4), 277–283.

15 K. M. Alananbeh, Z. Al-Qudah, A. El-Adly and W. J. Al Refaee, Impact of Silver Nanoparticles on Bacteria Isolated from Raw and Treated Wastewater in Madinah, KSA, *Arabian J. Sci. Eng.*, 2017, **42**(1), 85–93.

16 K. Alananbeh, W. Al-Refaee and Z. Al-Qodah, Antifungal effect of silver nanoparticles on selected fungi isolated from raw and waste water, *Indian J. Pharm. Sci.*, 2017, **79**(4), 559–567.

17 Z. Al-Qodah, M. Al-Shannag, K. Bani-Melhem, E. Assirey, K. Alananbeh and N. Bouqellah, Biodegradation of olive mills wastewater using thermophilic bacteria, *Desalin. Water Treat.*, 2015, **56**(7), 1908–1917.

18 M. S. Nejad, G. H. S. Bonjar, M. Khatami, A. Amini and S. Aghighi, *In vitro* and *in vivo* antifungal properties of silver nanoparticles against *Rhizoctonia solani*, a common agent of rice sheath blight disease, *IET Nanobiotechnol.*, 2017, **11**(3), 236–240, http://digital-library.theiet.org/content/journals/10.1049/iet-nbt.2015.0121.

19 M. Zarei, A. Jamnejad and E. Khajehali, Antibacterial Effect of Silver Nanoparticles Against Four Foodborne Pathogens, *Jundishapur J. Microbiol.*, 2014, **7**(1), e8720.

20 M. Khatami, N. Zafarnia, M. H. Bami, I. Sharifi and H. Singh, Antifungal and antibacterial activity of densely dispersed silver nanospheres with homogeneity size which synthesized using chicory: an in vitro study, *J. Mycolog. Med.*, 2018, **28**(4), 637–644.

21 P. Ponmurugan, Biosynthesis of silver and gold nanoparticles using *Trichoderma atroviride* for the biological control of *Phomopsis* canker disease in tea plants, *IET Nanobiotechnol.*, 2017, **11**(3), 261–267.

22 L. K. Foong, M. M. Foroughi, A. F. Mirhosseini, M. Safaei, S. Jahani, M. Mostafavi, *et al.*, Applications of nano-materials in diverse dentistry regimes, *RSC Adv.*, 2020, **10**(26), 15430–15460.

23 K. Mishra, N. Basavegowda and Y. R. Lee, AuFeAg hybrid nanoparticles as an efficient recyclable catalyst for the synthesis of α,β- and β,β-dichloroenones, *Appl. Catal., A*, 2015, **506**, 180–187.

24 S. Majidi, F. Zeinali Sehrig, S. M. Farkhani, M. Soleymani Goloujeh and A. Akbarzadeh, Current methods for synthesis of magnetic nanoparticles, *Artif. Cells, Nanomed., Biotechnol.*, 2016, **44**(2), 722–734.

25 Y. Pang, C. Wang, J. Wang, Z. Sun, R. Xiao and S. Wang, Fe_3O_4@Ag magnetic nanoparticles for microRNA capture and duplex-specific nuclease signal amplification based SERS detection in cancer cells, *Biosens. Bioelectron.*, 2016, **79**, 574–580.

26 K. Karthik, S. Dhanuskodi, C. Gobinath, S. Prabukumar and S. Sivaramakrishnan, Andrographis paniculata extract mediated green synthesis of CdO nanoparticles and its electrochemical and antibacterial studies, *J. Mater. Sci.: Mater. Electron.*, 2017, **28**(11), 7991–8001.

27 K. Karthik, S. Dhanuskodi, C. Gobinath, S. Prabukumar and S. Sivaramakrishnan, Ultrasonic-assisted CdO–MgO nanocomposite for multifunctional applications, *Mater. Technol.*, 2019, 1–12.

28 M. Khatami, I. Sharifi, M. A. L. Nobre, N. Zafarnia and M. R. Aflatoonian, Waste-grass-mediated green synthesis of silver nanoparticles and evaluation of their anticancer, antifungal and antibacterial activity, *Green Chem. Lett. Rev.*, 2018, **11**(2), 125–134.

29 B. Noorani, F. Tabandeh, F. Yazdian, Z.-S. Soheili, M. Shakibaie and S. Rahmani, Thin natural gelatin/chitosan nanofibrous scaffolds for retinal pigment epithelium cells, *Int. J. Polym. Mater. Polym. Biomater.*, 2018, **67**(12), 754–763.

30 M. Khatami, R. S. Varma, N. Zafarnia, H. Yaghoobi, M. Sarani and V. G. Kumar, Applications of green synthesized Ag, ZnO and Ag/ZnO nanoparticles for making clinical antimicrobial wound-healing bandages, *Sustainable Chem. Pharm.*, 2018, **10**, 9–15.

31 A. Miri, M. Sarani, A. Hashemzadeh, Z. Mardani and M. Darroudi, Biosynthesis and cytotoxic activity of lead oxide nanoparticles, *Green Chem. Lett. Rev.*, 2018, **11**(4), 567–572.

32 A. Toolabi, M. Malakootian, M. T. Ghaneian, A. Esrafili, M. H. Ehrampoush, M. AskarShahi, *et al.*, Optimizing the photocatalytic process of removing diazinon pesticide from aqueous solutions and effluent toxicity assessment *via* a response surface methodology approach, *Rendiconti Lincei. Sci. Fis. Nat.*, 2018, **30**, 155–165.

33 N. S. Seddighi, S. Salari and A. R. Izadi, Evaluation of antifungal effect of iron-oxide nanoparticles against different Candida species, *IET Nanobiotechnol.*, 2017, 883–888, http://digital-library.theiet.org/content/journals/10.1049/iet-nbt.2017.0025.

34 E. Zare, S. Pourseyedi, M. Khatami and E. Darezereshki, Simple biosynthesis of zinc oxide nanoparticles using nature's source, and it's in vitro bio-activity, *J. Mol. Struct.*, 2017, **1146**, 96–103.

35 O. Antonoglou, J. Moustaka, I. D. Adamakis, I. Sperdouli, A. A. Pantazaki, M. Moustakas, *et al.*, Nanobrass CuZn nanoparticles as foliar spray non phytotoxic fungicides, *ACS Appl. Mater. Interfaces*, 2018, **10**(5), 4450–4461.

36 P. Jamdagni, J. S. Rana, P. Khatri and K. Nehra, Comparative account of antifungal activity of green and chemically synthesized zinc oxide nanoparticles in combination with agricultural fungicides, *Int. J. Nano Dimens.*, 2018, **9**(2), 198–208.

